Journal of Advances in Medicine and Medical Research

33(12): 115-129, 2021; Article no.JAMMR.68754
ISSN: 2456-8899
(Past name: British Journal of Medicine and Medical Research, Past ISSN: 2231-0614, NLM ID: 101570965)

Determining the Dynamic Contrast - Enhanced Magnetic Resonance Imaging (DCE- MRI) in Diagnosis of Pulmonary Nodules

Mona Adel El-Nenaey[1*], Mohamed Mahmoud Alashwah[1], Basem Ibrahim Al-Shafey[2] and Amr Mohamed El-Badry[1]

[1]Departments of Radiology and Chest diseases, Tanta University, Tanta, Egypt.

Authors' contributions

This work was carried out in collaboration among all authors. All authors read and approved the final manuscript.

Article Information

DOI: 10.9734/JAMMR/2021/v33i1230948
Editor(s):
(1) Dr. Ashish Anand, GV Montgomery Veteran Affairs Medical Center,USA and University of Mississippi Medical Center,USA and William Carey School of Osteopathic Medicine, USA.
Reviewers:
(1) Adilio da S. Dadda, Instituto Nacional de Ciência e Tecnologia em Tuberculose, Brazil.
(2) Nilkanth Mukund Deshpande, Savitribai Phule Pune University, India.
Complete Peer review History: http://www.sdiarticle4.com/review-history/68754

Original Research Article

Received 18 March 2021
Accepted 28 May 2021
Published 02 June 2021

ABSTRACT

Objective: The aim of this study is to evaluate the role of dynamic contrast _ enhanced magnetic resonance imaging (DCE-MRI) in diagnosis of pulmonary nodules.
Patients and methods: The study was a cross-sectional study that was conducted on 30 patients with lung nodules referred to Radio diagnosis and imaging department from chest and oncology departments. By performing repeated CT within 30 days, we identified malignant nodules. The CT was repeated at 3 and 6 months which showed that the malignant pulmonary nodules increased in size and number.
Results: The maximum enhancement curve was a significant discriminator. At cut-off value of ≥ 375, the maximum enhancement curve yielded a sensitivity of 92.6% and specificity of 96% (figure 3). In contrary, the ADC value had poor diagnostic accuracy in differentiating between malignant and benign cases.
Conclusion: Dynamic contrast-enhanced MRI is valuable for diagnosis of pulmonary nodules and discrimination of benign from malignant ones.

**Corresponding author: E-mail: drmonaadel59@gmail.com;*

Keywords: Computed tomography; magnetic resonance imaging, positron emission tomography; national lung screening trial with sensitivity of 92.6% and specificity of 96%.

ABBREVIATIONS

CT	:	*Computed tomography*
MRI	:	*Magnetic resonance imaging*
DCE-MRI	:	*Dynamic contrast enhanced magnetic resonance imaging*
PET/CT	:	*Positron emission tomography combined with computed tomography*
DWI	:	*Diffusion weighted imaging*
ADC	:	*Apparent diffusion coeffient*
SI	:	*Signal intensity*
WFSE	:	*Weighted fast spin echo*
NLST	:	*National lung screening trial*
SPSS	:	*Statistical package for the social sciences*
Mmol	:	*Millimole*
Msec	:	*Millisecond*
IQR	:	*Interquartile range*
SD	:	*Standard deviation*
PPV	:	*Positive predictive value*
NPV	:	*Negative predictive value*
AUC	:	*Area under curve*
CI	:	*Confidence interval*

1. INTRODUCTION

The evaluation of pulmonary nodules is one of the most frequently encountered challenges in thoracic radiology [1].

The study of tumor neo angiogenesis is currently a leading theme in oncology; it has become challenging goal for radiologists to assess noninvasively the physiology of the tumor microcirculation, in addition to conventional morphology [2].

Angiogenesis is now extensively studied by dynamic contrast- enhanced (DCE) magnetic resonance imaging. Recent clinical studies have shown that DCE-MRI can assess tumor aggressiveness and measure tumor response to therapy [3].

Dynamic MRI has higher soft tissue contrast than CT and is useful for assessing tumor vascularity, interstitium, and vascular endothelial growth factor expression, and for predicting survival outcome among patients. These advantages make dynamic magnetic resonance imaging (MRI) ideal method for characterizing tumor response to anti-angiogenic treatment as well as for predicting survival outcomes after treatment in addition to non exposure to radiation [4].

Dynamic contrast enhanced imaging describes the acquisition of a base line images without contrast enhancement followed by a series of images acquired over time after intravenous bolus of contrast agent [5].

Dynamic contrast enhanced MRI is helpful in differentiating benign and malignant pulmonary nodules. Absence of significant enhancement is strong predictor that the lesion is benign [6].

The aim of this study is to evaluate the role of dynamic contrast _ enhanced magnetic resonance imaging (DCE-MRI) in diagnosis of pulmonary nodules.

2. PATIENTS & METHODS

The study was a cross-sectional study that was conducted on 30 patients with lung nodules referred to Radio diagnosis and imaging department from chest and oncology departments. The study was conducted through the period from September 2018 to September 2019.

Inclusion criteria: All patients enrolled in the study period were diagnosed having pulmonary nodules and all of them older than 18 years old.

Exclusion criteria: Patients with past history of previous allergy to contrast media were excluded.Also, patients who had metal implants were excluded. Patients those had impaired renal functional tests were postponed till their levels have been controlled.

Dynamic contrast-enhanced MRI: MR imaging was performed with a 1.0-T MR imager (Magnetom Expert; Siemens, Erlangen, Germany) by using the phased-array coil as the receiver. For lesion detection, the thorax was examined from the apex to the base by using a transverse breath-hold electrocardiographically gated proton-density-weighted twodimensional gradient-echo MR sequence (repetition time msec/echo time msec, 800–1,000/6; flip angle, 20°; voxel size, 1.3 x 1.3 x 6.0 mm).

Dynamic contrast-enhanced MR images were acquired in the sagittal plane every 10 seconds over a total period of 4 minutes by using a T1-weighted in-phase two-dimensional gradient-echo MR sequence (20/4.8; flip angle, 70°; voxel size, 1.4 x 1.4 x 8.0 mm). Sagittal dynamic imaging was performed across the maximal diameter of the nodule on transverse MR images. For every measurement, a short inspiratory breath-hold period of 4 seconds was required. Although expiratory breath holds are considered more reproducible, the images were acquired in inspiration because we assumed a better delineation of the lesion against enhanced vessels and inflated lung parenchyma, particularly in cases of small nodules. In contrast to transverse images, sagittal images can depict the nodule with all breath holds, even for slightly different inspiration levels, since the lateral to medial positional change of the nodules is minor.

Rapid bolus injection of a standard dose of 0.1 mmol per kilogram of body weight of gadopentetate dimeglumine [7], followed by 20 mL of 0.9% saline through a 21-gauge needle in an antecubital vein, was started at the time of acquisition of the second image (of a series of 24 images). All MR imaging examinations were completed within 25 minutes, including placement of the intravenous catheter. No adverse effects were observed.

Mean SIs of the lesions were measured on the operator console by a chest radiologist with 5 years of experience (J.V.), who placed a freehand region of interest that encompassed all of the cross-sectional visible area of the lesion at the 24 designated time points. Regions with few pixels could have larger SDs over time. That was investigated by means of simple linear regression from individual unconditional SDs in nodule size (percentage increase in SI [SI%] per centimeter). Visible pulmonary vessels beneath the lesion were excluded from the region of interest, which was adapted to movement of the lesion caused by different inspiration levels. Additionally, a circular region of interest with a size of 30 mm was placed in the lung lobe that contained the nodule and was analyzed to assess the enhancement of parenchyma and pulmonary vessels. All measurements were obtained without prior knowledge of the histologic diagnosis. SI% of nodules was determined for each time point (t) Time-intensity curves were plotted automatically for every lesion without any fitting.

The following parameters were evaluated. Early peak was determined as the highest SI% value in the first 30 seconds after t0. Maximum peak represented the maximum SI% value during the observation time. First transit slope represented the mean velocity SI increase per second from t0 to the time of early peak (EP) enhancement and was calculated. Washout phase was used to assess the changes in SI% per second for the 60- second time interval after the early peak. Mean enhancement represented the mean value of all measurements of SI%. After confirmation of lesion type by means of histologic examination or follow-up and classification of lesions as benign or malignant, medians and interquartile ranges were calculated for parameters of the time-intensity curves and nodule diameters. Medians of each time point of the time-intensity curves were calculated for both malignant and benign nodules to indicate location of values that were distributed abnormally.

Two radiologists experienced in chest radiology performed a retrospective morphologic analysis of contrast enhancement by means of consensus. The readers had no knowledge of histologic findings. Images of the time series were displayed in cine mode on the operator console. Five enhancement patterns were distinguishable: no enhancement, representing an absence of contrast material uptake in the lesion; homogeneous enhancement, representing uniform contrast material distribution; heterogeneous enhancement, representing irregular contrast enhancement with parts of no or low enhancement; nodular enhancement (hot spot– like), representing irregular enhancement with spotty high perfusion; and peripheral enhancement of capsular-like rim, representing smooth, thin, and uniform enhancement in the periphery of a round or ovoid lesion.

2.1 Statistical Analysis

An Excel spreadsheet was established for the entry of data. We used validation checks on

numerical variables and option-based data entry method for categorical variables to reduce potential errors. The analyses were carried with SPSS software (Statistical Package for the Social Sciences, version 24, SSPS Inc, Chicago, IL, USA). Frequency tables with percentages were used for categorical variables and descriptive statistics (median and interquartile range [IQR]) were used for numerical variables. Independent Student t-test, paired t-test, or Mann-Whitney tests were used to compare quantitative variables, while Chi-square test or McNemar-Bowker tests were used to analyze categorical variables. A p-value < 0.05 is considered statistically significant.

3. RESULTS

The mean age of the included patients was 53.27 ±10.6 years, while the majority of patients were females (56.7%). Sixty percent of the patients were older than 50 years old. In addition, 26.7% presented with metastatic breast cancer and 20% presented with metastatic cancer prostate. Three patients (10%) presented with metastatic cancer tail of pancreases, metastatic salivary tumor, dyspnea/hemoptysis, and unknown origin, each. The rest of the patients with sarcoma of left arm and thigh (Fig. 1). The mean serum creatinine and urea of the included patients was 0.863 ±0.21 and 20.97 ±6.88 mg/dL. The plain X-ray showed that 46.7% of the patients had bilateral scatter pulmonary nodules, 16.7% had suspected nodules, 10% had unilateral nodules, and 26.7% had normal findings. The MRI findings of the included patients showed that 46.7% of them had multiple nodules and 43.3% had single nodules; while 3 (10%) patients had two nodules. The site of the nodules was bilateral (46.7%), right upper lung lobe (20%), right lower lung lobe (10%), left middle lung lobe (10%), left lower lung lobe (6.7%), and left middle lung lobe (6.7%). Table (1)

The mean maximum net enhancement was 474 ±94.417 and slope of enhancement was 186.3 ±138. The MRI showed that the mean ADC value was 1.2 ±0.34 x 10.3 mm^2/sec and the enhancement curve was 62 ±11.7 HU. The mean washout ratio was 5.45 ±2.17%. The pattern of enhancement was homogenous in 50% of cases, heterogeneous in 40%, marginal in 6.7%, and non-enhanced in 3.3% of cases. Table (2), Fig. (2).

There were statistically significant differences between malignant and benign cases in terms of maximum net enhancement (p =0.003) and ADC value (p <0.001). Malignant cases had significantly higher maximum net enhancement, washout ratio, and lower ADC value. There was no statistically significant differences between malignant and benign cases in terms of type of enhancement (p =0.42). Table (3).

Diagnostic performance of ADC value and maximum enhancement curve in differentiating between malignant and benign cases. The maximum enhancement curve was a significant discriminator. At cut-off value of ≥ 375, the maximum enhancement curve yielded a sensitivity of 92.6% and specificity of 96% (Fig. 3). In contrary, the ADC value had poor diagnostic accuracy in differentiating between malignant and benign cases. Table (4)

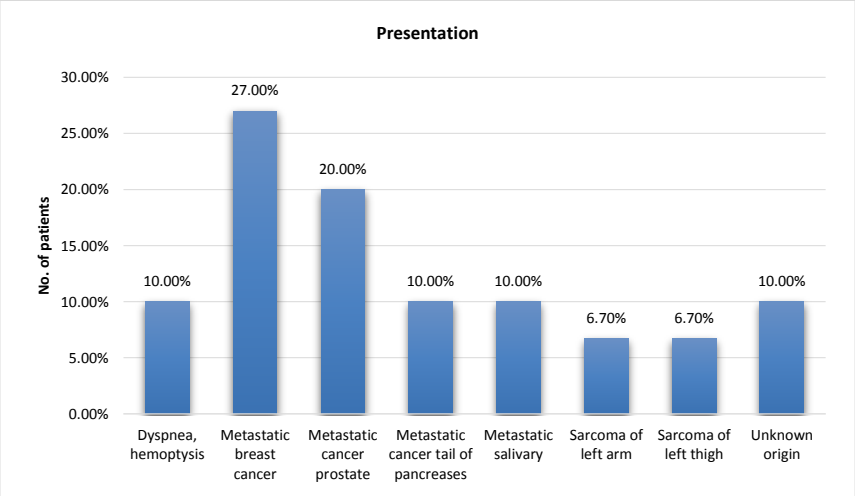

Fig. 1. Presentation of the included patients

Table 1. Baseline demographic characteristics of the included patients

Variables		Patients (N =30)	
		No	%
Age in years		53.27 ±10.6	
	Mean ±SD	- 52 (42 – 62)	
	Median (IQR)	-	
Age group40-50		12	40
	>50-60	- 9	30
	>60-70	- 9	30
Gender			
	Male	- 13	43.3
	Female	- 17	56.7
Presentation			
	Dyspnea, hemoptysis	- 3	10.0
	Metastatic breast cancer	- 8	26.7
	Metastatic cancer prostate	- 6	20.0
	Metastatic cancer tail of pancreases	- 3	10.0
	Metastatic salivary	- 3	10.0
	Sarcoma of left arm	- 2	6.7
	Sarcoma of left thigh	- 2	6.7
	Unknown origin	- 3	10.0
Serum creatinine (mg/dL)		0.863 ±0.21	
	Mean ±SD	- 0.8 (0.7 – 1)	
	Median (IQR)	-	
Serum urea (mg/dL)		20.97 ±6.88	
	Mean ±SD	- 20 (16 – 22)	
	Median (IQR)	-	
Plain X-ray Findings			
	Bilateral scattered nodules	- 14	46.7
	Normal	- 8	26.7
	Suspected	- 5	16.7
	Unilateral nodule	- 3	10.0
Number of nodules			
	Multiple	- 14	46.7
	Single	- 13	43.3
	Two	- 3	10.0
Site of nodules			
	Bilateral	- 14	46.7
	Left lower lung lobe	- 2	6.7
	Left middle lung lobe	- 3	10.0
	Left upper lung lobe	- 2	6.7
	Right Lower lung lobe	- 3	10.0
	Right upper lung lobe	- 6	20.0

4. CASES

Case 1

- Clinical history: 70 years old male known case of metastatic cancer prostate.

X-ray examination: unremarkable study.
Laboratory investigations: creatinine 0.9mg/dl urea 20mg/dl.

MRI finding (Fig. 4)**:** right upper lung lobe solitary pulmonary nodule with speculated margin measures about (1.4x1 cm) seen displacing isointense signal at T1 (A) &T2 (B), in addition to pretracheal LN about 1 cm. While after dynamic post contrast phases that lasts for 4 minutes the nodule showing homogenous enhancement at arterial phase (C) and washout at portal (D)and delayed (E) phases. ADC value is 0.9x10-3 mm2/s with restricted diffusion (F) (nodule is bright). The time-enhancement curve is of type A (G). CT examination showed solitary pulmonary nodule with speculated margin measures about (1.5x1 cm) seen at right upper lung lobe then after 3 months CT examination was done as follow up and the nodule was stationary but after another 3 months, the nodule

showed progressive course regarding the size to be (2x1.3 cm) and number to be other few smaller nodules appeared bilaterally.

Case 2

Clinical history: 62 years old male known case of metastatic cancer prostate.

X-ray examination: suspected pulmonary nodules seen at right lower lung zone.

Laboratory investigations: creatinine 1.3mg/dl urea 21mg/dl.

MRI finding (Fig 5)**:** two pulmonary nodules seen at right lower lung lobe, the largest measures about (2.2x1.8 cm) and the other measures (1.5x1 cm), the nodules seen displacing isointense signal at T1 (A)&T2 (B). While after dynamic post contrast phases that lasts for 4 minutes the nodules showing arterial enhancement (C) and washout at subsequent phases (D&E). ADC value is 1.2x10-3 mm2/s with restricted diffusion (F) (nodules are bright). The time-enhancement curve is of type B (G). CT examination revealed two pulmonary nodules seen at right lower lung lobe, largest measures about 2.3x2 cm, after 3 months the size increased to 2.6x2.4 cm then after another 3 months the size became 3x2.5 cm and other tiny nodules appeared at the other side.

Case 3

Clinical history: 41 years old male case of old TB infection complaining of dyspnea and hemoptysis.

X-ray examination: bilateral pulmonary nodules seen scattered at both lung fields.

Laboratory investigations: creatinine 0.8mg/dl urea 14mg/dl.

MRI finding (Fig. 6)**:** few bilateral pulmonary nodules the largest seen at right upper lung lobe measures about (1.8x1.6 cm), the nodules showing isointense signal at T1 (A)&T2 (B). While after dynamic post contrast phases that lasts for 4 minutes the nodules showing faint arterial enhancement (C) with persistent enhancement at subsequent phases (no washout)(D&E). ADC value is 2x10-3 mm2/s with no evidence of restricted diffusion (F). The time-enhancement curve is of type C (G). CT examination revealed few bilateral calcified pulmonary nodules largest seen at right upper lung lobe measures about 2x1.8 cm representing old granulomatous infection.

Table 2. MRI findings of the included patients

Variables		Patients (N =30)	
		No	%
Max. net enhancement			
	Mean ±SD	- 474 ± 94.417	
	Median (IQR)	- 450 (400 – 550)	
Slope of enhancement			
	Mean ±SD	- 186.3 ±138	
	Median (IQR)	- 100 (100 – 300)	
Washout ratio			
	Mean ±SD	- 5.45 ±2.17	
	Median (IQR)	- 6 (0 – 12)	
Enhancement curve HU			
	Mean ±SD	- 62 ±11.7	
	Median (IQR)	- 60 (36–92)	
Type of curve			
	A	- 24 (80%)	
	B	- 4 (13.3%)	
	C	- 2 (6.7%)	
ADC value x 10.3 mm^2/sec			
	Mean ±SD	- 1.2 ± 0.34	
	Median (IQR)	- 1.2 (0.76 – 2)	
Type of enhancement			
	Homogenous	- 15	50
	Heterogeneous	- 12	40
	Marginal	- 2	6.7
	Non-enhanced or faint	- 1	3.3

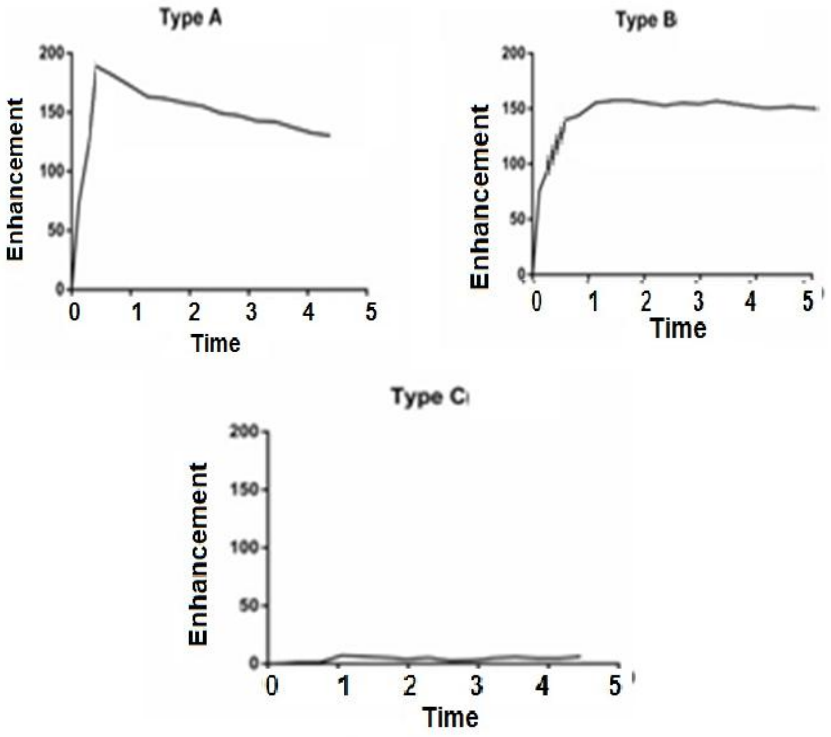

Fig. 2. Types of time –enhancement curve [8]

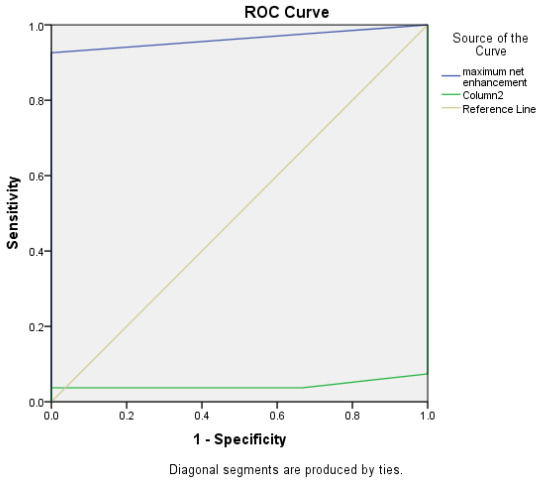

Fig. 3. The area under the curve and the diagnostic accuracy of ADC value and maximum enhancement curve in differentiating between malignant and benign cases

5. DISCUSSION

The incidental finding of lung nodule(s) in asymptomatic individuals is an increasingly common clinical dilemma encountered by radiologists and pulmonologists in daily clinical practice. Accurate identification and characterization of malignant lung nodules and development of clear algorithms for their management, permitting cure of early-stage lung cancer while avoiding morbidity, patient distress and increased costs caused by more invasive and unwarranted for benign disease approaches, remain a challenge [9].

Table 3. MRI findings according to pathology

Variables			Malignant (N =27)	Benign (N =3)	P-value
Max. net enhancement					
	Mean ±SD	-	487.78 ± 89	350 ± 89	0.003
Washout ratio					
	Mean ±SD	-	5.82 ±1.28	4.01 ±2.39	0.04
	Median (IQR)	-	6 (3 – 12)	4 (3 – 10)	
ADC value x 10.3 mm^2/sec					
	Mean ±SD	-	1.14 ± 0.47	1.9 ± 0.1	<0.001
Type of enhancement					
	Homogenous	-	12 (44.4%)	3 (100%)	
	Heterogeneous	-	12 (44.4%)		0.42
	Marginal	-	2 (7.4%)		
	Non-enhanced or faint	-	1 (3.7%)		

Table 4. The area under the curve and the diagnostic accuracy of ADC value and maximum enhancement curve in differentiating between malignant and benign cases

Variable	AUC, 95% CI	P- value	Cut-off points	Sensitivity	Specificity	PPV	NPV
ADC value	0.05 (0.01-0.11)	0.01	NA	NA	NA	NA	NA
Washout ratio	NA	NA	NA	NA	NA	NA	NA
Max. net enhancement	0.96(0.89-0.99)	0.011	≥ 375	92.6%	96%	86.2%	81.5%

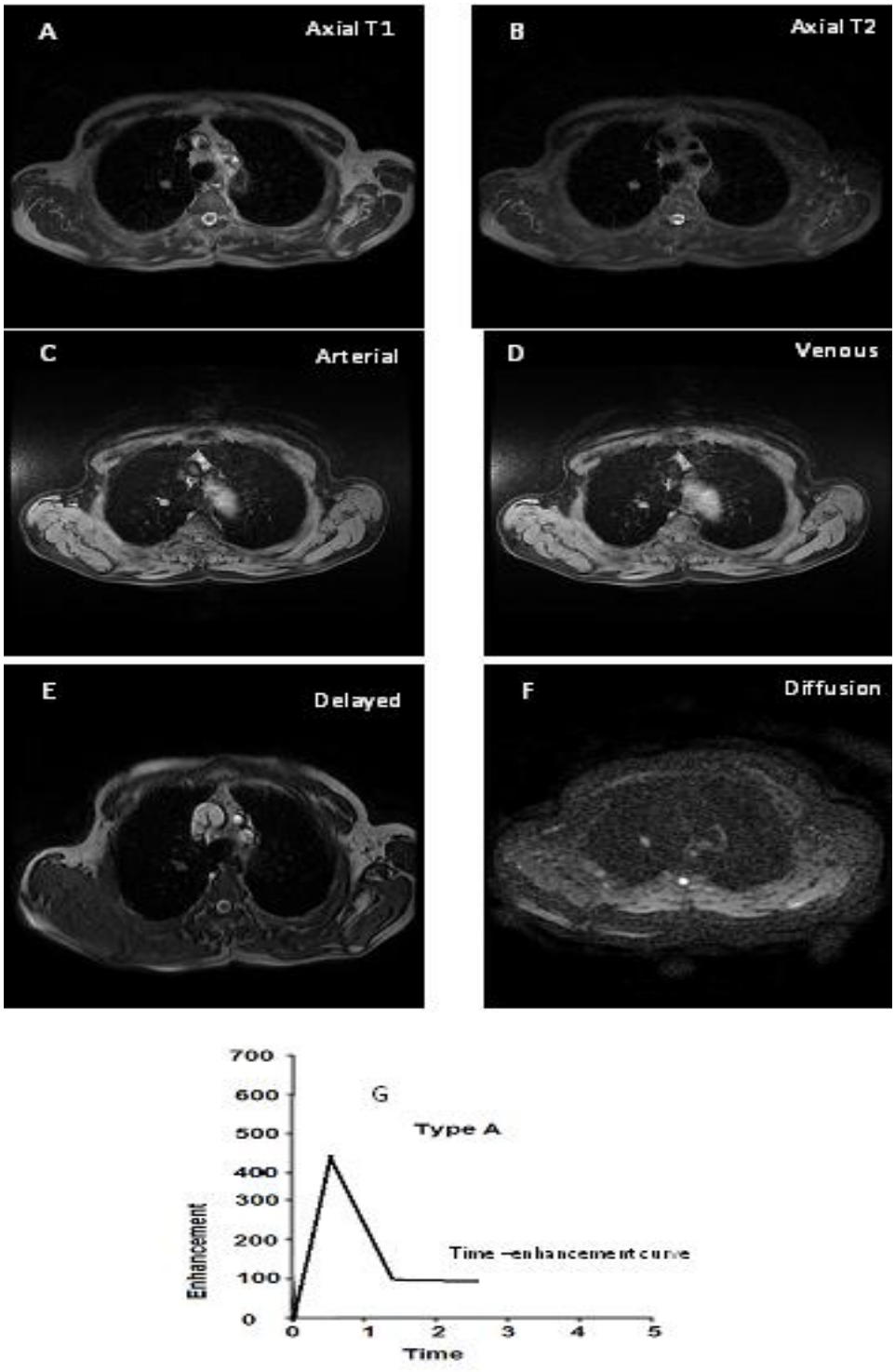

Fig. 4. Case number 1. Right upper lung lobe solitary pulmonary nodule with speculated margin measures about (1.4x1 cm) seen displacing isointense signal at T1 (A) &T2 (B), in addition to pretracheal LN about 1 cm. While after dynamic post contrast phases that lasts for 4 minutes the nodule showing homogenous enhancement at arterial phase (C) and washout at portal (D)and delayed (E) phases. ADC value is 0.9x10-3 mm2/s with restricted diffusion (F) (nodule is bright). The time-enhancement curve is of type A (G). CT examination showed solitary pulmonary nodule with speculated margin measures about (1.5x1 cm) seen at right upper lung lobe

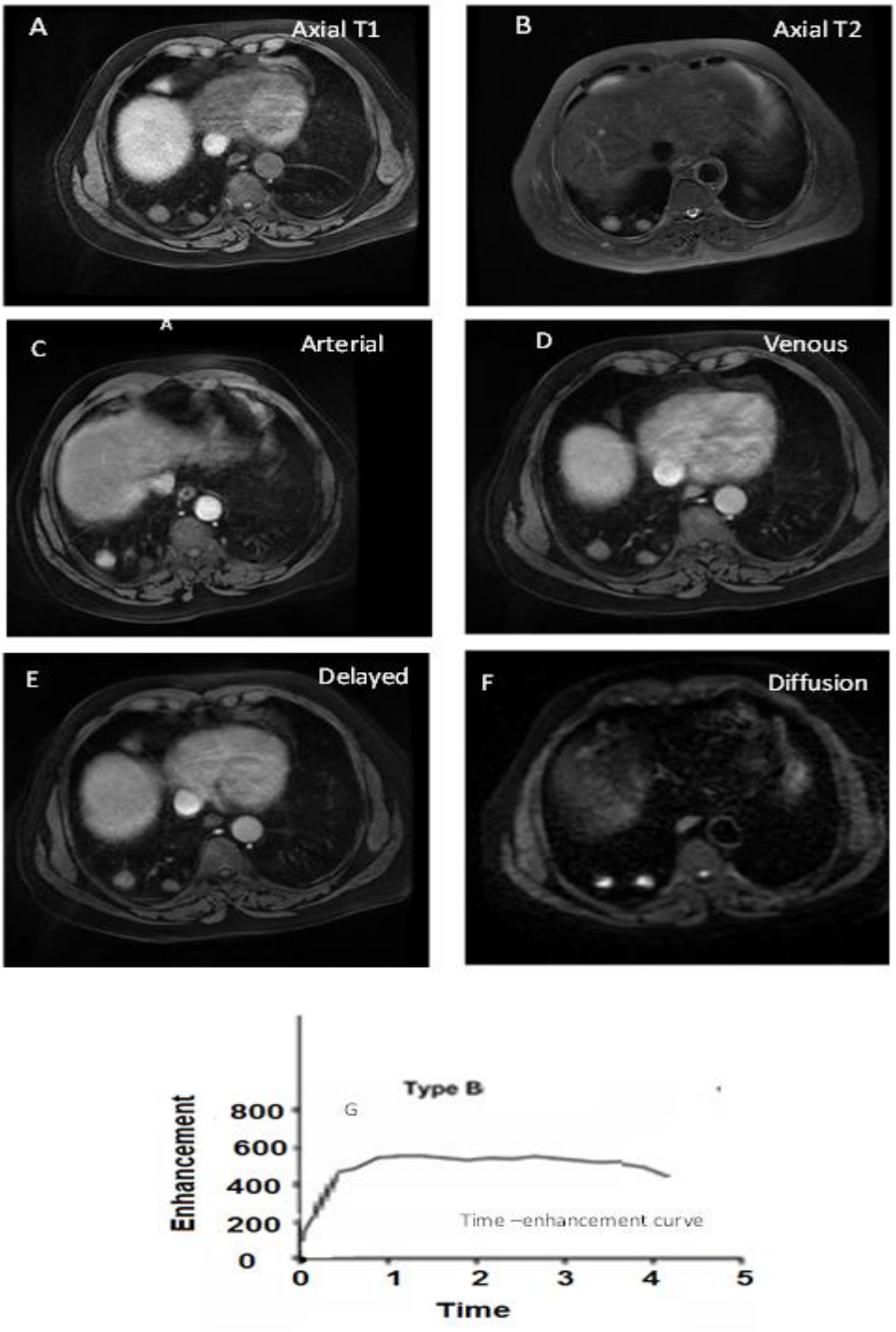

Fig. 5. Case number 2. Two pulmonary nodules seen at right lower lung lobe, the largest measures about (2.2x1.8 cm) and the other measures (1.5x1 cm), the nodules seen displacing isointense signal at T1 (A)&T2 (B). While after dynamic post contrast phases that lasts for 4 minutes the nodules showing arterial enhancement (C) and washout at subsequent phases (D&E). ADC value is 1.2x10-3 mm2/s with restricted diffusion (F) (nodules are bright). The time-enhancement curve is of type B (G). CT examination revealed two pulmonary nodules seen at right lower lung lobe, largest measures about 2.3x2 cm, after 3 months the size increased to 2.6x2.4 cm then after another 3 months the size became 3x2.5 cm and other tiny nodules appeared at the other side

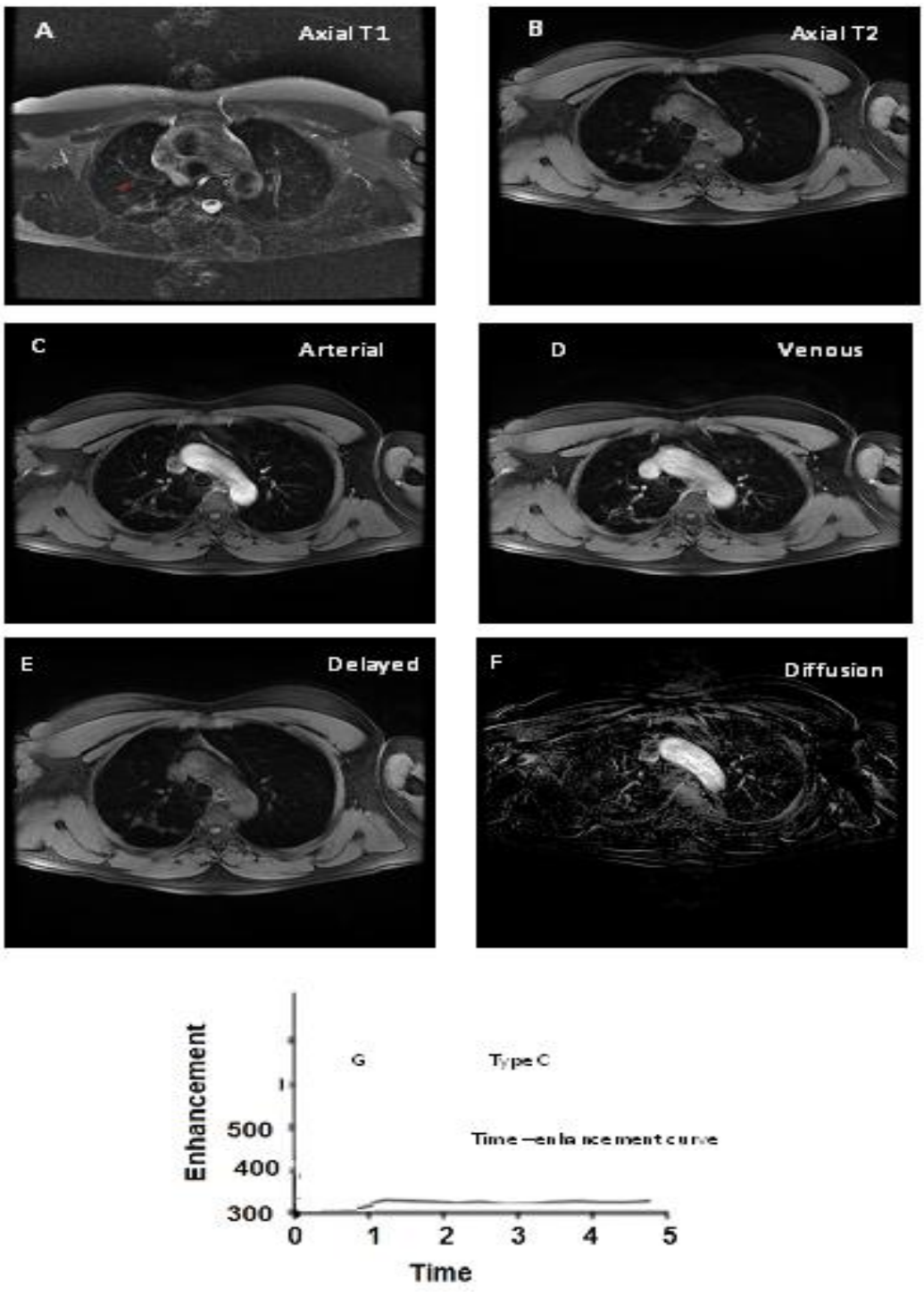

Fig. 6. Case number 3. Few bilateral pulmonary nodules the largest seen at right upper lung lobe measures about (1.8x1.6 cm), the nodules showing isointense signal at T1 (A)&T2 (B). While after dynamic post contrast phases that lasts for 4 minutes the nodules showing faint arterial enhancement (C) with persistent enhancement at subsequent phases (no washout)(D&E). ADC value is 2x10-3 mm2/s with no evidence of restricted diffusion (F). The time-enhancement curve is of type C (G). CT examination revealed few bilateral calcified pulmonary nodules largest seen at right upper lung lobe measures about 2x1.8 cm representing old granulomatous infection

After detecting a lung nodule, the main goal for physicians is to identify a nodule suspicious enough to warrant further testing as early as possible, but avoiding unnecessary diagnostic or therapeutic procedures. In cases of malignant nodules, the early diagnosis of lung cancer could provide a safe and definitive solution. In this context, detection and follow-up using a computed tomography (CT) play an important role. However, there is a risk of false-positive results with CT, in addition to the biological cost in terms of radiation burden from several CT scans required during follow-up and healthcare costs [10].

Over the past few decades, magnetic resonance imaging (MRI) of pulmonary nodules has emerged as an alternative for CT. Since the early 1990s, many investigators have used contrast-enhanced MRI and dynamic contrast-enhanced MRI to evaluate the radiologic features, with promising results. The advantage of using dynamic contrast-enhanced MRI in tumor characterization has been reported by several researchers. Sequences with short acquisition times enable the assessment of the first bolus transit in tumor perfusion [11].

Nevertheless, there is a scarcity in the published literature regarding the diagnostic utility of dynamic contrast-enhanced MRI for detection of malignant pulmonary nodules. Therefore, we conducted the present cross-sectional study in order to evaluate the role of dynamic contrast-enhanced MRI for the diagnosis of pulmonary nodules.

The study was a cross-sectional study that was conducted on 30 patients with lung nodules referred to Radio diagnosis and imaging department from chest and oncology departments. The study was conducted through the period from September 2018 to September 2019.

Previous epidemiological studies have shown that pulmonary nodules are commonly detected after the age of 45 years [12].

In our cohort, The mean age of the included patients was 53.27 ±10.6 years, while 60% of the patients were older than 50 years old. The majority of patients were females (56.7%). The female predominance in the present study can be attributed to a large number of patients with breast cancers. An additional explanation is the notable higher incidence of malignant nodules in our study, previous reports showed that female gender is a predictor of malignancy in cases presented with pulmonary nodules [13].

In line with our findings, **Yang and colleagues** [13] retrospectively analyzed the clinical and imaging data of patients with pulmonary nodules who underwent computer tomography-guided needle biopsy from Jan 2011 to March 2016. A total of 1422 consecutive patients were enrolled with a mean age of 55.41 ± 11.94 years.

Similarly, **Shi and colleagues** [14] analyzed the role of the sizes of solitary pulmonary nodules in predicting their potential malignancies. A total of 379 patients with pathologically confirmed nodules were enrolled in this study. The mean age of the included patients was 51.17±13.79 years, with a slight female predominance.

Regarding nodules' characteristics, we found that 46.7% of the patients had multiple nodules and 43.3% had single nodules. The site of the nodules was bilateral in 46.7% of the cases.

Likewise, **Azhar and colleagues** [15] performed a retrospective study to analyze the patient profile nodule characteristics of incidentally found pulmonary nodule.135 patients with incidental nodule(s) were referred to the service where 325 nodules were reviewed. The majority of patients had multiple, bilateral, nodules.

In addition, **Caparica and colleagues** [16] conducted a retrospective, single-institution study that included consecutive patients with nonpulmonary solid malignancies who underwent biopsy from January 2011 to December 2013. Of 146 patients, 51% of them had multiple nodules.

After detecting a lung nodule, the main goal for physicians is to identify a nodule suspicious enough to warrant further testing as early as possible, but avoiding unnecessary diagnostic or therapeutic procedures. In cases of malignant nodules, the early diagnosis of lung cancer could provide a safe and definitive solution. In this context, detection and follow-up using computed tomography (CT) play an important role. Nodule size and growth rate remain the most widely used predictors to assess probability of nodule malignancy and to determine nodule management according to the international guidelines [10].

In the present study, nodule growth, determined by imaging surveillance, was used as a

diagnostic tool for assessing malignancy. By performing repeated CT within 30 days, we idenified malignant nodules. The CT was repeated at 3 and 6 months which showed that the malignant pulmonary nodules increased in size and number.

In terms of the primary outcomes of the present study, the results showed that the dynamic contrast-enhanced MRI showed that 86.7% of pulmonary nodules were malignant nodules; while there was one case with bronchogenic carcinoma. The CT showed that 96.7% of the pulmonary nodules were malignant nodules. The dynamic contrast-enhanced MRI achieved a sensitivity of 93.1% and a specificity of 100% for the detection of malignant pulmonary nodules.

In concordance with our findings, **Jianga and colleagues** [11] performed a metaanalysis to assess the diagnostic performance and clinical utility of the dynamic MRI in discrimination of benign and malignant pulmonary nodules. The authors searched PubMed, EMBASE, and Cochrane Library from January 1995 to May 2015 for studies evaluating the diagnostic accuracy of dynamic MRI in discriminating benign from malignant pulmonary nodules. Twelve studies with 524 malignant and 284 benign nodules were included in this metaanalysis. The sensitivity and specificity of MRI was 95 and 87%, respectively.

Rapid and strong contrast enhancement is related to high vascularity in tumors and interstitial accumulation of contrast material by means of increased permeability of tumor capillaries. These features are often present in malignant tumors. In contrast to the iodinated contrast material in CT examinations, the paramagnetic contrast material effects in MRI depend additionally on the interactions of mobile water molecules in all tissue compartments, including the interstitium and cytoplasm. In addition, versatile parameters determined from signal intensity–time course curves can improve the diagnostic accuracy [17].

In the present study, there were statistically significant differences between malignant and benign cases in terms of maximum net enhancement (p =0.003) and washout (p =0.04). Malignant cases had significantly higher maximum net enhancement and washout ratio. At cut-off value of ≥ 375, the maximum enhancement curve yielded a sensitivity of 92.6% and specificity of 96%.

Similarly, **Alper and colleagues** [18] aimed to assess the use of dynamic MRI in the management of pulmonary nodules. Thirty-one patients were included; of which, 16 (52%) were malignant. These showed a stronger enhancement with higher median values of early peak and maximum peak than those corresponding to the benign lesions. There were significant differences between the benign and malignant lesions ($p < 0.001$). Sensitivity, specificity, positive predictive value and negative predictive value were 75, 93, 92 and 78% for EP and 93, 86, 88 and 93% for MP, respectively.

Moreover, **Schaefer and colleagues** [19] aimed to determine whether dynamic contrast–enhanced MRI reveals statistically significant differences between malignant and benign solitary pulmonary nodules. Fifty-eight patients were included and the frequency of malignancy was 53% (27 of 51 nodules). Malignant nodules showed stronger enhancement with a higher maximum peak and a faster slope (P <.001). Significant washout (>0.1% increase in signal intensity per second) was found only in malignant lesions (14 of 27 lesions). Sensitivity, specificity, and accuracy were 96%, 88%, and 92%, respectively, for maximum peak; 96%, 75%, and 86% for slope; and 52%, 100%, and 75% for washout. When curve profiles and morphologic enhancement patterns were combined, sensitivity increased to 100%.

Kim and colleagues [20] performed a prospective study to compare the diagnostic performances of dynamic MR imaging and CT for the differentiation of benign and malignant solitary pulmonary nodules. Eighty-one patients with nodules (32 malignant, 49 benign) underwent dynamic MR imaging. The malignant nodules revealed significantly greater degrees of peak enhancement on dynamic MR imaging.

Ohno and colleagues [21] prospectively compare the capabilities of dynamic perfusion area-detector computed tomography (CT), dynamic MRI, and positron emission tomography (PET) combined with CT (PET/CT) with use of fluorine 18 fluorodeoxyglucose (FDG) for the diagnosis of solitary pulmonary nodules. A total of 198 consecutive patients with 218 nodules prospectively underwent dynamic perfusion area-detector CT, dynamic MR imaging, FDG PET/CT, and microbacterial and/or pathologic examinations. The maximum relative enhancement ratio and slope of enhancement ratio showed significant differences between

malignant nodules and benign nodules. The area under the receiver operating characteristic curve for maximum relative enhancement ratio and slope of enhancement ratio was high.

Nevertheless, other reports showed lower diagnostic performance of MRI than our study. For example, Kono and colleagues [22] compared the dynamic contrast-enhanced MRI enhancement characteristics of malignant and benign solitary pulmonary nodules. The characteristics of 202 solitary pulmonary nodules were reviewed retrospectively. With 110% or lower maximum enhancement ratio as a cutoff value, the positive predictive value for malignancy was 92%; sensitivity, 63%; and specificity, 74%.

The exact causes of such heterogeneity are unclear. However, this difference can be attributed to different population's characteristics, small sample size, or methodological differences.

The present study has some limitations. The sample size of the included patients was relatively small and from a single center which may limit the possibility that the study's results can be generalized to the general population

6. CONCLUSION

Dynamic contrast-enhanced MRI is valuable for diagnosis of pulmonary nodules and help in discrimination of benign from malignant ones. Moreover, dynamic MRI delineates significant kinetic and morphologic differences in vascularity and perfusion between malignant and benign solitary pulmonary nodules. The maximum net enhancement seems to be highly specific for malignancy Nevertheless, further studies are still needed to confirm our findings.

CONSENT

As per international standard or university standard, patients' written consent has been collected and preserved by the author(s).

ETHICAL APPROVAL

As per international standard or university standard written ethical approval has been collected and preserved by the author(s).

COMPETING INTERESTS

Authors have declared that no competing interests exist.

REFERENCES

1. Soon H, Chang M, Sang J et al. Radiology. 2016;280(3)940-948.
2. Nagihan I, Arzu A, Muhammed D, et al. Iranian Journal of Radiology. 2016;13(2):111-115.
3. Doenja MJ, Monique M, Marcel PM et al. seminars in radiology oncology. 2016;26(3):193-198.
4. David CP, Hans CJ,Rob H et al. Technology in cancer research & Treatment. 2016,15(6):47-60.
5. Kazuhiro L, yoshihiro M, Hajime S et al. Surgery to day 2014;44(7):1197-1206.
6. Feng F, Fulil Q, Aijul S et al. Chinese journal of cancer research. 2018;30(1)21-25.
7. Knopp MV, Bourne MW, Sardanelli F, Wasser MN, Bonomo L, Boetes C, et al. Gadobenate dimeglumine-enhanced MRI of the breast: analysis of dose response and comparison with gadopentetate dimeglumine. AJR Am J Roentgenol. 2003;181:663-76.
8. Mona A, Mohamad M, Al-shafey BA, AMR T. Dynamic Contrast-Enhanced Magnetic Resonance Imaging (DCE-MRI) in Diagnosis of Pulmonary Nodules. The Medical Journal of Cairo University. 20201;88(June):1193-202.
9. Loverdos K, Fotiadis A, Kontogianni C. et al. Lung nodules: A comprehensive review on current approach and management. Annals of Thoracic Medicine. Wolters Kluwer Medknow Publications; 2019.
10. Larici AR, Farchione A, Franchi P, et al. Lung nodules: Size still matters. European Respiratory Review. 2017;26(146).
11. Jiang B, Liu H, Zhou D. (a). Diagnostic and clinical utility of dynamic contrast-enhanced MR imaging in indeterminate pulmonary nodules: A metaanalysis. Clinical Imaging. 2016;40(6):1219–1225.
12. Gould MK, Donington J, Lynch WR, et al. Evaluation of Individuals With Pulmonary Nodules: When Is It Lung

Cancer? Chest. 2013;143(5):e93S – e120S.

13. Yang L, Zhang Q, Bai L, et al. Assessment of the cancer risk factors of solitary pulmonary nodules. Oncotarget. 2017;8(17):29318–29327.
14. Shi CZ, Zhao Q, Luo LP, et al. Size of solitary pulmonary nodule was the risk factor of malignancy. Journal of Thoracic Disease. 2014;6(6):668–676.
15. Azhar A, Hussain A, Islam S, et al. Profile and nodule characteristics of patients with incidental subsolid pulmonary nodules (SSN). In. 2016;PA3810.
16. Caparica R, Mak MP, Rocha CH, et al. Pulmonary Nodules in Patients With Nonpulmonary Cancer: Not Always Metastases. Journal of Global Oncology. 2016; 2(3):138–144.
17. Ohno Y, Nishio M, Koyama H, et al. Dynamic contrast-enhanced CT and MRI for pulmonary nodule assessment. American Journal of Roentgenology; 2014.
18. Alper F, Kurt ATP, Aydin Y, et al. The role of dynamic magnetic resonance imaging in the evaluation of pulmonary nodules and masses. Medical Principles and Practice. 2012; 22(1):80–86.
19. Schaefer JF, Vollmar J, Schick F, et al. Solitary pulmonary nodules: Dynamic contrast-enhanced MR imaging - Perfusion differences in malignant and benign lesions. Radiology. 2004; 232(2):544–553.
20. Kim JH, Kim HJ, Lee KH, et al. Solitary pulmonary nodules: A comparative study evaluated with contrast-enhanced dynamic MR imaging and CT. Journal of Computer Assisted Tomography. 2004;28(6):766–775.
21. Ohno Y, Nishio M, Koyama H, et al. Solitary pulmonary nodules: Comparison of dynamic first-pass contrast-enhanced perfusion area-detector CT, dynamic first-pass contrast-enhanced MR imaging, and FDG PET/CT. Radiology. 2015; 274(2):563–575.
22. Kono R, Fujimoto K, Terasaki H, et al. Dynamic MRI of solitary pulmonary nodules: Comparison of enhancement patterns of malignant and benign small peripheral lung lesions. American Journal of Roentgenology; 2007.

Peer-review history:
The peer review history for this paper can be accessed here:
http://www.sdiarticle4.com/review-history/68754